Biochimica et Biophysica Acta 1802 (2010) 462–471

Contents lists available at ScienceDirect

Biochimica et Biophysica Acta

journal homepage: www.elsevier.com/locate/bbadis

Increased SOD1 association with chromatin, DNA damage, p53 activation, and apoptosis in a cellular model of SOD1-linked ALS

Livea F. Barbosa [a], Fernanda M. Cerqueira [a], Antero F.A. Macedo [a], Camila C.M. Garcia [a], José Pedro F. Angeli [a], Robert I. Schumacher [a], Mari Cleide Sogayar [a], Ohara Augusto [a], Maria Teresa Carrì [b,c], Paolo Di Mascio [a], Marisa H.G. Medeiros [a,*]

[a] Departamento de Bioquímica, Instituto de Química, Universidade de São Paulo, São Paulo, Brazil
[b] Department of Biology, University of Rome "Tor Vergata", Italy
[c] Fondazione Santa Lucia IRCCS, Rome, Italy

ARTICLE INFO

Article history:
Received 4 September 2009
Received in revised form 23 December 2009
Accepted 15 January 2010
Available online 25 January 2010

Keywords:
ALS
SOD1
p53
Nucleus
DNA damage

ABSTRACT

Mutations in the gene encoding cytosolic Cu,Zn-superoxide dismutase (SOD1) have been linked to familial amyotrophic lateral sclerosis (FALS). However the molecular mechanisms of motor neuron death are multifactorial and remain unclear. Here we examined DNA damage, p53 activity and apoptosis in SH-SY5Y human neuroblastoma cells transfected to achieve low-level expression of either wild-type or mutant $Gly^{93} \rightarrow Ala$ (G93A) SOD1, typical of FALS. DNA damage was investigated by evaluating the levels of 8-oxo-7,8-dihydro-2′-deoxyguanosine (8-oxodGuo) and DNA strand breaks. Significantly higher levels of DNA damage, increased p53 activity, and a greater percentage of apoptotic cells were observed in SH-SY5Y cells transfected with G93A SOD1 when compared to cells overexpressing wild-type SOD1 and untransfected cells. Western blot, FACS, and confocal microscopy analysis demonstrated that G93A SOD1 is present in the nucleus in association with DNA. Nuclear G93A SOD1 has identical superoxide dismutase activity but displays increased peroxidase activity when compared to wild-type SOD1. These results indicate that the G93A mutant SOD1 association with DNA might induce DNA damage and trigger the apoptotic response by activating p53. This toxic activity of mutant SOD1 in the nucleus may play an important role in the complex mechanisms associated with motor neuron death observed in ALS pathogenesis.

1. Introduction

Amyotrophic lateral sclerosis (ALS) is a neurodegenerative disease characterized by progressive loss of motor neurons, leading to muscle atrophy, paralysis, and death [1,2]. The majority of cases are sporadic with unknown causes, but around 10% are familial inherited forms (FALS) [3]. About 25% of FALS cases are associated with mutations in the gene encoding cytosolic Cu,Zn-superoxide dismutase (SOD1), a very abundant antioxidant enzyme in the central nervous system [4]. Currently, more than a hundred point mutations in the *sod1* gene have been found in FALS patients [5]; however, the reason these mutations cause motor neuron death remains an unanswered question. There is no clear correlation between enzyme activity, clinical progression, and disease phenotype, since most mutants retain full catalytic activity [6,7]. The $Gly^{93} \rightarrow Ala$ (G93A) mutation is one of the most studied mutations worldwide due to the availability of G93A SOD1 transgenic animals [8]. Mice and rats overexpressing human G93A SOD1, as well as other FALS mutations, develop very similar features to ALS patients, with progressive motor neuron degeneration, reviewed in [9], while SOD1 knockout mice do not develop motor neuron disease [10]. The autosomal dominant nature of SOD1-associated FALS suggests a toxic gain of function for the mutant enzyme. Currently, it is known that FALS-linked SOD1 mutants tend to form toxic aggregates and cause oxidative molecular damage and mitochondrial dysfunction, consequently triggering apoptosis in neuronal cells, reviewed in [11]. The toxicity of mutant SOD1 seems to precede aggregation [12–14], and may be explained by its increased ability to promote the oxidation of biomolecules. SOD1-mediated oxidation can occur via its peroxidase activity, reviewed in [15] but its role in ALS remains controversial. The unambiguous fact is that accumulation of oxidatively generated damage to proteins, lipids, and DNA occurs in ALS patients and in SOD1 G93A animal models, reviewed in [16].

The toxicity of FALS-mutant SOD1 has been largely associated with its recruitment to mitochondria [17–19], leading to respiratory failure [20,21] and activation of the apoptotic cascade [22,23]. A recent study

Abbreviations: SOD1, Cu,Zn-superoxide dismutase; ALS, amyotrophic lateral sclerosis; FALS, familial amyotrophic lateral sclerosis; dGuo, 2′-deoxyguanosine; 8-oxodGuo, 8-oxo-7,8-dihydro-2′-deoxyguanosine; MDA, malondialdehyde; TBA, 2-thiobarbituric acid; HPLC, high-performance liquid chromatography; EC, electrochemical detection; ER, endoplasmic reticulum; NBT, nitro blue tetrazolium; DHR, dihydrorhodamine

* Corresponding author. Departamento de Bioquímica, Instituto de Química, Universidade de São Paulo, Av. Prof. Lineu Prestes 748, CEP 05508-900, São Paulo, SP, Brazil. Tel.: +55 11 30912153; fax: +55 11 30912186.
E-mail address: mhgdmede@iq.usp.br (M.H.G. Medeiros).

0925-4439/$ – see front matter © 2010 Elsevier B.V. All rights reserved.
doi:10.1016/j.bbadis.2010.01.011

showed that mutant SOD1 can also trigger apoptosis by promoting endoplasmic reticulum (ER) stress [24,25]. Nuclear apoptotic mechanisms have been less explored. Nuclear p53 protein triggers apoptosis as a consequence of the accumulation of DNA damage [26], but the mechanism underlying this phenomenon is not fully understood. p53 is phosphorylated and subsequently activated by the ataxia–telangiectasia mutated (ATM) protein upon binding to a DNA double-strand break. Activated p53 upregulates the *bax* pro-apoptotic gene and inhibits the *bcl-2* anti-apoptotic gene [27]. The response to other forms of DNA damage that generates single-stranded regions is coordinated mainly by ataxia–telangiectasia and Rad3-related protein kinases (ATR). ATR associates with claspin and phosphorylates downstream substrates including p53 [28]. Increased levels of p53 were found in ALS patients and animal models [29–31], but a direct relationship between p53 levels and DNA damage has never been sought. Increased levels of 8-oxo-7,8-dihydro-2′-deoxyguanosine (8-oxodGuo), a product of DNA oxidation, were found in the spinal cord and motor cortex of ALS patients [33–35]. Furthermore, increased levels of free 8-oxodGuo in the urine, plasma, and cerebrospinal fluid of ALS patients correlated with disease progression and severity [36].

In the present work, we examined dismutase and peroxidase SOD1 activity in total cellular and nuclear extracts obtained from SH-SY5Y human neuroblastoma cells transfected with either wild-type SOD1 or the G93A FALS-mutant SOD1. SOD1 peroxidase activity positively correlated with DNA damage in these cells, as assessed by the levels of 8-oxodGuo as well as by strand break formation. p53 activity and apoptosis were also evaluated in these cells. Our results demonstrate a toxic activity for mutant SOD1 in the nucleus, indicating that DNA damage may play an important role in the pathogenesis of ALS.

2. Materials and methods

2.1. Chemicals

All the chemicals employed in the present study were of the highest commercially available purity grade. Chromatography grade methanol, formic acid, chloroform, ethanol, and 2-chloroacetaldehyde were acquired from Merck (Darmstadt, Germany). Hydrogen peroxide was from Fluka Chemika (Buchs, Switzerland). Fetal bovine serum and Dulbecco's MEM-HAM F12 medium were purchased from Cultilab (Campinas, Brazil). Deferoxamine mesylate salt was from Ciba-Geigy (Basel, Switzerland). Geneticin was from Gibco (Paisley, UK). All other chemicals were from Sigma (St. Louis, MO). Water was purified using a Milli-Q system (Millipore, Bedford, MA).

2.2. Cell culture

SH-SY5Y human neuroblastoma cells were purchased from the European Collection of Cell Culture and grown at 37 °C in Dulbecco's MEM-HAM F12 supplemented with 15% fetal calf serum, 3.7 g/L sodium bicarbonate, 40 mg of penicillin/L, and 100 mg of streptomycin/L in an atmosphere of 5% CO_2 in air. Clonal cell lines transfected with either human wild-type SOD1, G93A or H46R mutants SOD1 were obtained as previously described [37]. Cells lines were selected by treatment with 200 mg/L geneticin, which was removed 2 days before performing the experiments.

2.3. Cell treatment

The medium from confluent cultures was replaced with fresh medium and 0.5 mM H_2O_2 was then added. After incubating for 2 h, the medium was removed and the assays were performed. In order to analyze lipid peroxidation, the culture medium was replaced with Hanks solution prior to addition of 0.5 mM H_2O_2. After the incubation period, both the culture medium and the cells from each plate were transferred to tubes and subjected to the procedure described below for malondialdehyde determination.

2.4. Malondialdehyde (MDA) determination

After cell treatment, 7 mL of a 0.4% (w/v) solution of 2-thiobarbituric acid (TBA) in HCl 0.2 N/H_2O (2:1) and 1 mL of a 0.2% (w/v) solution of butylated hydroxytoluene in 95% ethanol were added to the samples and the mixture was heated to 90 °C for 45 min, cooled on ice, and extracted with isobutanol. The isobutanolic phase was injected through a Shimadzu auto injector model SIL-10AD/VP (Shimadzu, Kyoto, Japan) in a Shimadzu HPLC system, consisting of two LC-6AD pumps connected to a Lichrosorb 10 RP-18 (Phenomenex, Torrance, CA) reversed-phase column (250 mm × 4.6 mm i.d. particle size 10 μm). The flow rate of the isocratic eluent (25 mM potassium phosphate buffer pH 7 with 40% of methanol) was 1 mL/min. An RF-10A/XL fluorescence detector was set at an excitation wavelength of 515 nm and an emission wavelength of 550 nm. The data were processed using Shimadzu Class-VP 5.03 software. Malonaldehyde-bisdiethylacetal was used for calibration of the fluorescence data, yielding a quantitative adduct of the malonaldehyde-TBA product. The data were expressed as pmol of MDA normalized to the protein content (in μg).

2.5. Comet assay

After treatment of the cells with H_2O_2 (0.5 mM), approximately 10^4 cells were suspended in 0.5% low-melting-point agarose in PBS at 37 °C and placed on a glass microscope slide coated with a layer of 1.5% normal-melting-point agarose in PBS. The slides were immersed in cold-lysing solution (2.5 M NaCl, 100 mM EDTA, 10 mM Tris–HCl pH 10, 10% dimethylsulfoxide, 1% Triton X-100) for 120 min at 4 °C. The slides were incubated for 45 min at 37 °C with 1 U Formamidopyrimidine DNA glycosylase (Fpg) or Endonuclease III (Endo III). After enzyme digestion, the slides were placed in an electrophoresis tank immersed in ice, allowing the DNA to unwind for 20 min in alkaline solution (300 mM NaOH and 1 mM EDTA, pH > 13). Electrophoresis was then carried at 300 mA, 25V, for 20 min in the same solution. The slides were neutralized with 0.4 M Tris–HCl buffer (pH 7.4), fixed in 100% ethanol and stained with ethidium bromide (20 μg/mL). Image analysis was performed by fluorescence microscopy using a Diaphot 300 (Nikon, Tokyo, Japan) with a 510–560 nm filter and a 590 nm barrier. Fifty comets on each slide were visually analyzed using a Komet 6.0 software. The results were expressed as tail intensity.

2.6. DNA extraction from cultured cell

The cells (4×10^7 cells) were centrifuged at 1500 × *g* for 10 min and each pellet was suspended in 3 mL of lysis solution 1% (w/v) Triton X-100, 320 mM sucrose, 5 mM $MgCl_2$, 10 mM Tris–HCl, pH 7.5). This step was repeated once and, after centrifugation at 1500 × *g* for 10 min, the nuclear pellets were suspended in 3 mL of 10 mM Tris–HCl buffer pH 8.0 containing 5 mM EDTA and 0.15 mM deferoxamine. The enzymes RNase A (30 μL of a 10 g/L solution in 10 mM AcONa pH 5.2, heated for 15 min at 100 °C), and RNase T1 (4 μL of a 20 U/μL solution in 10 mM Tris–HCl buffer, pH 7.4 containing 1 mM EDTA and 2.5 mM deferoxamine) were added together with 200 μL of a 10% (w/v) solution of SDS, and the reaction mixture was incubated at 37 °C for 1 h. After incubation, 60 μL of proteinase K (20 g/L) was added, followed by an additional incubation at 37 °C for 1 h. After centrifugation at 5000 × *g* for 15 min, the liquid phase was collected and 2 mL of 40 mM Tris–HCl buffer, pH 8 containing 7.6 M NaI, 20 mM EDTA and 0.3 mM deferoxamine were added to the cells, followed by the addition of 4 mL of isopropanol. The tube contents were mixed well by inversion until a whitish precipitate formed. The precipitate was collected by centrifugation at 5000 × *g* for 15 min and washed with 1 mL of 60% isopropanol (v/v), followed by 1 mL of 70% ethanol (v/v). After an additional centrifugation at 5000 × *g* for 15 min,

the DNA pellet was solubilized in a 0.1 mM solution of deferoxamine. The DNA concentration was measured spectrophotometrically at 260 nm, and its purity was assessed by ensuring an $A_{260}/A_{280} \geq 1.7$ using a UV-1650PC spectrophotometer (Shimadzu, Kyoto, Japan).

2.7. Enzymatic hydrolysis of DNA

Hydrolysis of 100 μg of DNA was performed by addition of 2.0 μL of 1 M sodium acetate buffer, pH 5.0 and 1 U of nuclease P_1 followed by incubation at 37 °C for 30 min. After this incubation period, 4 μL of 1 M Tris–HCl, buffer pH 7.4 and 4 μL of 500 mM potassium acetate buffer, pH 7 containing 100 mM Tris-acetate and 100 mM magnesium acetate were added, followed by addition of 3 U of alkaline phosphatase. The reaction mixture was incubated at 37 °C for 1 h. The final volume of the sample was adjusted to 100 μL with water. The enzymes were precipitated by immediate addition of one volume of chloroform at the end of the hydrolysis. After centrifugation at 1000×*g* for 5 min, the resulting aqueous layer was subjected to analysis. The DNA amounts subjected to hydrolysis were 100 μg for analysis of 8-oxodGuo.

2.8. Analysis of 8-oxodGuo using high-performance liquid chromatography/electrochemical detection (HPLC/EC)

Samples (100 μg) of digested DNA were injected into the HPLC/EC system, which consisted of a Shimadzu model LC-10 AD pump (Shimadzu, Tokyo, Japan) connected to a Luna C18 analytical column (250 mm×4.6 mm i.d., 5 μm) (Phenomenex, Torrance, CA) maintained at 16 °C by a CTO-10AS VP column oven (Shimadzu, Tokyo, Japan). The isocratic eluent was 25 mM potassium phosphate buffer pH 5.5 and 8% methanol at a flow rate of 1 mL/min. Coulometric detection was provided by a Coulochem II detector (ESA, Chelmsford, MA), and spectrophotometric detection by a Shimadzu SPD-10A (Shimadzu, Tokyo, Japan). The potential of the electrode was set at 280 mV for detection of 8-oxodGuo. Elution of unmodified nucleosides was simultaneously monitored by a Shimadzu SPD-10AV/VP UV detector set at 254 nm. The Shimadzu Class-LC10 1.6 software was used to calculate the peak areas. The molar ratio of 8-oxodGuo to 2′-deoxyguanosine (dGuo) in each DNA sample was determined based on coulometric detection at 280 mV for 8-oxodGuo and absorbance at 254 nm for dGuo in each injection.

2.9. Apoptosis

Apoptosis was measured by quantification of sub-diploid nuclei (sub-G_1events) [38]. Briefly, neuroblastoma cells (2×10^6 cells) in control conditions or after treatment with 0.5 mM H_2O_2 for 2 h were detached with trypsin and centrifuged at 1500×*g* for 5 min. The cell pellet was resuspended in 400 μL of fluorescent hypotonic solution (0.1% sodium citrate, 0.1% Triton X-100, 50 μg/mL propidium iodide). After 10 min, the cells were analyzed with a flow cytometer. Alternatively, the annexin VFITC assay was used to detect cells in apoptosis. Cell suspensions were washed with annexin binding buffer (10 mM HEPES, 150 mM NaCl, 5 mM KCl, 1 mM $MgCl_2$, 1,8 mM $CaCl_2$). Supernatants were removed and 100 μL annexin binding buffer with fluorescein isothiocyanate (FITC)-conjugated annexin-V (1 μM) was added to each pellet. Cells were stained for 40 min in the dark at room temperature. Immediately before collection, 400 μL of annexin binding buffer was added to each sample. Cells were analyzed with a flow cytometer (FACScalibur-Becton Dickinson, San Jose, CA). Fluorescence was quantified using the Facs Express 2.0 software.

2.10. Transient transfection of neuroblastomas for analysis of p53 activity using the reporter gene assay (luciferase activity)

Cells were grown in 24-well plates (10^5 cells/well) one day before transfection. A total amount of 0.2 μg of DNA was used for each well (0.16 μg of p53-luc vector (Strategene, La Jolla, CA) and 0.04 μg of pRL-TK vector, used as a control for transfection efficiency). The p53-Luc vector contains the luciferase gene with a promoter that is responsive to active p53. The pRL-TK vector contains the gene for renilla luciferase under the thymidine kinase promoter. FuGene 6 (Roche, Indianapolis, IN) was used as the transfection agent, and was diluted in DMEM-Ham F12 medium (0.6 μL of FuGene 6 per 20 μL of medium per well). The vectors were added to the diluted FuGene 6 and incubated for 15 min prior to addition of the mixture to cells. After 24 h, the medium was replaced and the cells were treated with 0.5 mM H_2O_2 for 2 h. The cells were lysed with PLB buffer (Promega, Madison, WI), and the activity of luciferase and renilla luciferase reporter genes was quantified using a luminometer (Micro Lomat Plus) and the Promega System (Dual-Luciferase Reporter Assay System).

2.11. Immunohistochemistry

Cells were seeded in 35-mm plates containing a glass coverslip (MatTek, Ashland, MA), fixed with paraformaldeyde (4%) for 15 min at room temperature and permeabilized with 0.1% Triton X-100. The samples were blocked for 1 h in 1% BSA in PBS and incubated for 2 h at 37 °C with sheep monoclonal anti-SOD1 antibody (Calbiochem, Darmstadt, Germany), and then washed in blocking buffer and incubated for 2 h with a goat anti-sheep antibody conjugated to Texas Red (Invitrogen, Eugene OR). After rinsing in PBS, the cells were stained with 10 μg/mL DAPI (Invitrogen-Molecular Probes, Eugene OR). The same protocol was performed for nuclear images, except for the permeabilization step. All images were acquired with a Zeiss LSM 510 Confocal Microscope.

2.12. Isolation and flow cytometry analysis of nuclei

The medium was removed from each plate and the cells were collected after trypsinization in calcium-free PBS. After centrifugation, the cell pellet was resuspended in 1 mL of lysis buffer (320 mM sucrose, 5 mM $MgCl_2$, 1% (w/v) Triton X-100, 1 mM Tris–HCl, pH 7.8) and incubated at 4 °C for 10 min. Nuclei were collected by centrifugation at 3300×*g* for 15 min, and resuspended in 1 mL of incubation buffer (320 mM sucrose, 5 mM $MgCl_2$, 0.1% (w/v) Triton X-100, 1 mM Tris–HCl, pH 7.8). Nuclei were incubated for 2 h at 37 °C with sheep monoclonal anti-SOD1 antibody (Calbiochem, Darmstadt, Germany). After incubation, the nuclei were washed and resuspended in incubation buffer containing goat anti-sheep antibody conjugated to Texas Red and incubated for 2 h (Invitrogen, Eugene OR). The presence of SOD1 was analyzed by flow cytometry using a Beckman Coulter FC500 MPL and MXP software.

2.13. Isolation and fractionation of nuclei

The medium was removed from each plate, and the cells were collected in PBS. After centrifugation, the cell pellet was resuspended in 100 μL of lysis buffer (100 mM NaCl, 300 mM sucrose, 3 mM $MgCl_2$, 1 mM EGTA, 10 mM NaF, 10 mM Pipes, 0.5% Triton X-100 (v/v), 1.2 mM PMSF, 1 μg/mL aprotinin, 5 μg/mL leupeptin, 1 μg/mL pepstatin) and incubated at 4 °C for 10 min. Nuclei were collected by centrifugation at 3300×*g* for 15 min. The supernatant was separated and, after 2 washes in lysis buffer, the nuclear pellet was resuspended in 100 μL of nuclear lysis buffer (0.5% (w/v) sodium deoxycholate, 10 mM NaCl, 3 mM $MgCl_2$, 10 mM NaF, 10 mM Tris, 1% Tween 20 (v/v), 1.2 mM PMSF, 1 μg/mL aprotinin, 5 μg/mL leupeptin, 1 μg/mL pepstatin). Soluble nuclear proteins were separated from the chromatin by centrifugation at 20,000×*g* for 5 min. After 2 washes in nuclear lysis buffer, the chromatin fraction was incubated in 50 μL of digestion buffer (50 mM NaCl, 300 mM sucrose, 3 mM $MgCl_2$, 1 mM EGTA, 10 mM NaF, 10 mM Pipes, 0.5% Triton X-100 (v/v), 1.2 mM PMSF, 1 μg/mL aprotinin, 5 μg/mL leupeptin, 1 μg/mL pepstatin,

30 U/50 µL DNase I, 50 µg/mL RNase A) for 1 h at 20 °C. Ammonium sulfate (5 µL of a 2.5 M solution) was added to dissociate the proteins from the DNA. After incubating for 5 min at room temperature, the chromatin-associated proteins were separated by centrifugation at 20,000×*g* for 10 min. The protein content of each fraction was then quantified.

2.14. Immunoblotting for SOD1, histone H1, and c-Fos

Nuclear-enriched protein fractions from SH-SY5Y cells were subjected to 15% SDS-PAGE and transferred to a nitrocellulose membrane by electroelution. Blots were blocked with 5% nonfat dry milk in TBS-T (0.05% Tween 20 in 50 mM Tris–HCl (pH 7.4), 150 mM NaCl) and incubated overnight with a sheep polyclonal antibody specific for human SOD1 (Calbiochem, Darmstadt, Germany) at 10 µg/mL in 0.1% nonfat dry milk TBS-T. After the primary antibody incubation, the blots were washed and incubated with peroxidase-conjugated secondary antibody (10 ng/mL) (Calbiochem, Darmstadt, Germany). The signal was developed using X-ray film and the SuperSignal West Pico Chemiluminescent Substrate kit (Pierce Biotechnology, Rockford, IL). Immunoblots for histone-H1 and c-Fos were subsequently performed in this order to assess the efficiency for the nuclear isolation and fractionation protocol and to normalize for protein loading. After overnight washing in TBS-T, the membrane was subjected to overnight incubations in TBS-T containing 0.1% nonfat dry milk and 1 µg/mL of a mouse monoclonal antibody specific for human histone-H1 (Upstate), followed by incubation with 2.5 µg/mL of a mouse monoclonal antibody specific for human c-Fos (Calbiochem, Darmstadt, Germany). Incubation with the proper peroxidase-conjugated secondary antibodies (10 ng/mL) (Calbiochem, Darmstadt, Germany) was then carried out.

2.15. Superoxide dismutase activity in cytosolic and nuclear protein extracts

Superoxide dismutase activity was assessed by spectrophotometric analysis. Reactions were incubated at 37 °C in 50 mM sodium carbonate pH 10.2 with 100 µM diethylenetriaminepentaacetic acid (DTPA), 100 µM xanthine, 56 µM nitro blue tetrazolium (NBT), 1 U/mL of catalase and xanthine oxidase to obtain an NBT reduction speed of 0.0120 ± 0.0002 Abs/min. NBT reduction was followed at 560 nm using a UV-1650PC spectrophotometer (Shimadzu, Kyoto, Japan). SOD1 activity was quantified by inhibition of NBT reduction in the presence of cytosolic and nuclear protein extracts (1–80 µg of total protein/mL). Cytosolic SH-SY5Y cells protein extracts were obtained by freeze-thawing. Nuclei were isolated using the method described above, and then subjected to freeze-thawing to liberate nuclear proteins.

2.16. Peroxidase activity in cytosolic and nuclear protein extracts

Cytosolic SH-SY5Y cells protein extracts were obtained by freeze-thawing. Nuclei were isolated using the method described above, and then subjected to freeze-thawing to liberate nuclear proteins. Cytosolic protein extracts (100 µg) and nuclear protein extracts (10 µg) were incubated with 80 µM dihydrorhodamine (DHR), 100 µM DTPA, and 3 mM H_2O_2 in sodium phosphate buffer, pH 6.8 in the absence or presence of 25 mM sodium bicarbonate. DHR oxidation to rhodamine was followed at 500 nm for 5 min at 37 °C using a UV-1650PC spectrophotometer (Shimadzu, Kyoto, Japan). The speed of enzymatic DHR oxidation was obtained from the linear coefficient of the plots.

2.17. Statistical analyses

Statistical analysis was performed by One-Way Analysis of Variance (ANOVA) followed by the Student–Newman–Keuls Multiple Comparison as a post-test. Values were considered statistically significant when $p < 0.05$.

3. Results

3.1. SH-SY5Y cells expressing G93A SOD1 demonstrate higher levels of DNA damage and lipid peroxidation

SH-SY5Y cells transfected with G93A SOD1 (G93A) displayed 2-fold increase in DNA strand breaks compared to control SH cells or cells transfected with wild-type SOD (WT), as evidenced by the increased damage index obtained in the comet assay (Fig. 1A). Addition of enzyme (Fpg or Endo III) significantly increased the level of DNA strand breaks in G93A cells, an effect which was not evidenced in the control cell neither in the wild-type SOD1. For comparative purposes, experiments with another model of FALS SOD1 mutant (H46R) cells, lacking SOD activity, were also performed. These H46R cells showed higher levels of DNA damage, however, the DNA damage displayed by H46R cell DNA is less sensitive to Fpg or Endo III enzymes than that of G93A cells (Fig. 1A). Treatment with H_2O_2 increased the tail intensity of all studied cells (Fig. 1B).

The basal levels of 8-oxodGuo in the DNA of G93A cells were 3-fold higher (~60 8-oxodGuo/10^7 dGuo) than those of SH and WT cells (~20 8-oxodGuo/10^7 dGuo). H_2O_2 treatment caused no significant difference in 8-oxodGuo levels in the DNA of SH and WT cells, but caused a 2-fold increase in the level of 8-oxodGuo in DNA of G93A cells (Fig. 2). Moreover, higher levels of MDA (a classical marker of lipid peroxidation) were also observed in G93A cells when compared

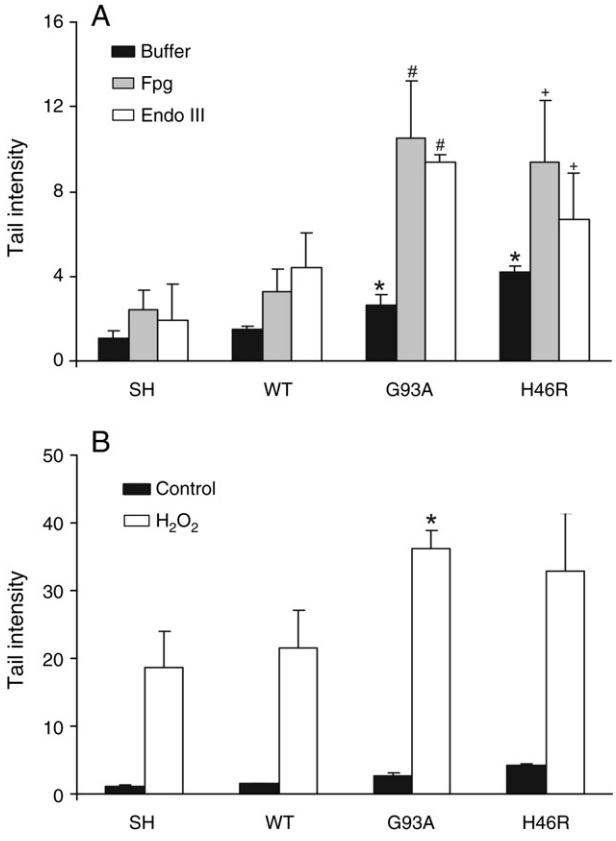

Fig. 1. A) Level of DNA strand breaks in genomic DNA of parental SH-SY5Y cells (SH), and cells transfected with wild-type SOD1 (WT), G93A mutant SOD1 (G93A) and H46R mutant SOD1 (H46R), under control conditions and upon treatment with 1 U of Fpg or Endo III. B) Level of DNA strand breaks in genomic DNA of SH-SY5Y cells and upon treatment with 0.5 mM of H_2O2 for 2 h. *Significantly different from SH and WT under the same condition, #significantly different from G93A under control conditions and +significantly different from H46R under control conditions ($p < 0.001$).

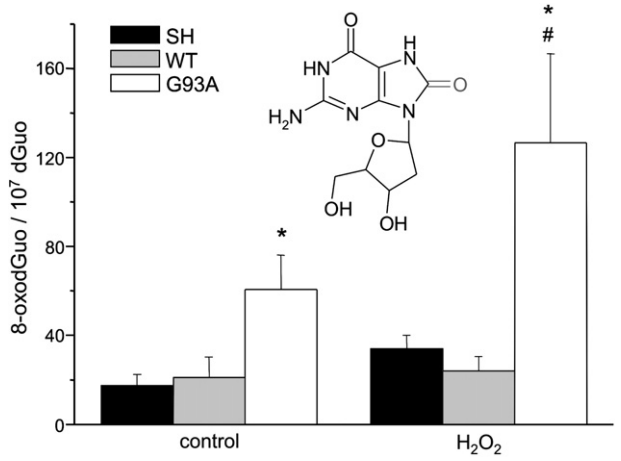

Fig. 2. Levels of 8-oxodGuo in genomic DNA of parental SH-SY5Y cells (SH), and of cells transfected with the wild-type SOD1 (WT) or the G93A mutant SOD1 (G93A), under control conditions and after treatment with 0.5 mM H_2O_2 for 2 h. *Significantly different from SH and WT under the same condition; #significantly different from G93A under control conditions ($p<0.001$). Inset: molecular structure of 8-oxodGuo linked to a 2-deoxyribose residue.

to SH and WT cells. A greater increase in MDA levels was also observed in the mutant cells upon H_2O_2 treatment (Fig. 3).

3.2. SH-SY5Y cells expressing G93A SOD1 display increased levels of apoptosis and p53 activity

Accumulation of DNA damage and p53-activated apoptotic cell death was evaluated in G93A, WT and SH cells. The involvement of p53 in activation of the apoptotic process was assessed by quantifying its activity, irrespective of the level of p53 protein in the cells compared to WT and control SH cells. G93A cells displayed increased (3-fold) of p53 activity (Fig. 4A). A ca. 3-fold increase was also observed in the levels of apoptosis measured by sub-G1 events (PI) (Fig. 4B) and by phosphatidylserine translocation (annexin-V assay) (Fig. 4C) when compared to WT and control SH cells. Hydrogen peroxide treatment did not alter p53 activity in any of these cell types neither apoptotic cell death in WT and control SH cells (Fig. 4A and C). After H_2O_2 treatment

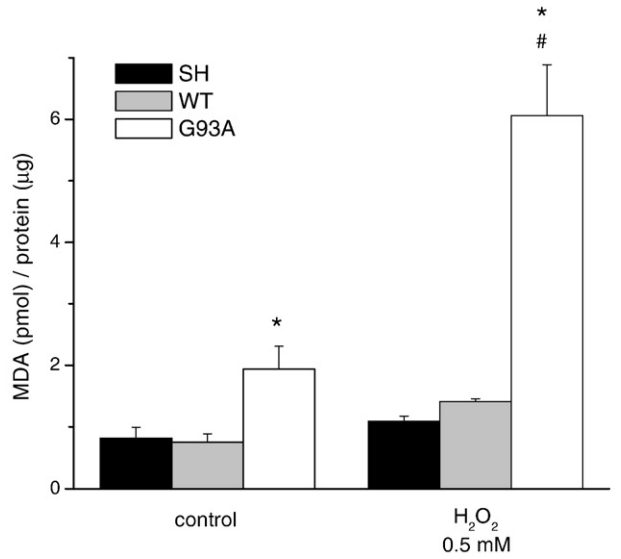

Fig. 3. Levels of lipid peroxidation determined by MDA present in cellular extracts obtained from parental SH-SY5Y cells (SH), and from cells transfected with the wild-type SOD1 (WT) or the G93A mutant SOD1 (G93A), under control conditions and after treatment with 0.5 mM H_2O_2 for 2 h. *Significantly different from SH and WT under the same condition; #significantly different from G93A under control conditions ($p<0.001$).

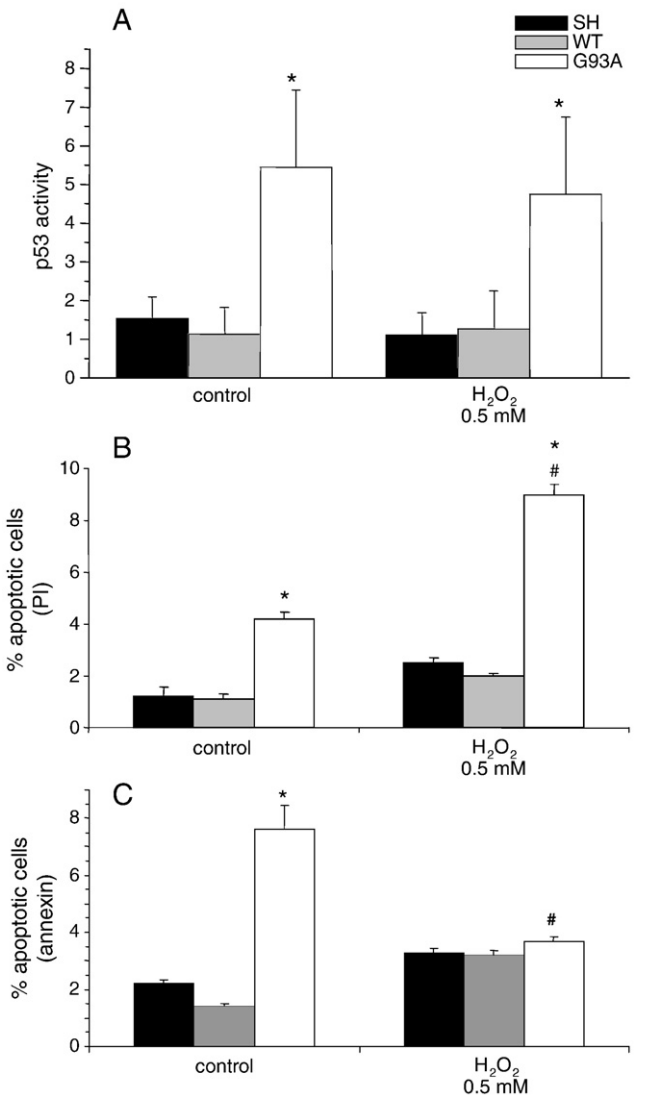

Fig. 4. Activity of p53 (A), apoptosis levels measured by sub-G1 population (PI) (B) and by phosphatidylserine translocation of parental SH-SY5Y cells (SH), and of cells transfected with the wild-type SOD1 (WT) or the G93A mutant SOD1 (G93A), under control conditions and after treatment with 0.5 mM H_2O_2 for 2 h. *Significantly different from SH and WT under the same condition; #significantly different from G93A under control conditions ($p<0.001$).

an increase in sub-G1 population was observed in G93A cells, since this increase was not observed by the annexin-V assay, it appears that cell death, in this case, occurs by necrosis (Fig. 4 B and C).

3.3. SH-SY5Y cells expressing G93A SOD1 exhibit increased levels of SOD1 associated with chromatin

The presence of SOD1 in the nucleus of mammalian cells has been previously described [39–41], suggesting that it may be a mediator of DNA oxidation. In accordance, we confirmed the presence of SOD1 in the nuclei of SH-SY5Y cells by FACS and confocal microscopy (Fig. 5). Furthermore, SOD1 immunoblots showed that control cells (SH) and cells transfected with wild-type SOD1 (WT) and mutant G93A SOD1 (G93A) display SOD1 in the nucleus, as a soluble protein (Fig. 6). Glucose 6-phosphatase activity was not detected in the nuclear fractions, indicating that no cytosolic contamination occurred. Transformed cell types (G93A, H46R and WT) displayed higher amounts of SOD1 in the nucleus than control SH cells, probably due to the double expression of SOD1 in the mutant cells [37]. Sau et al. [42] showed that G93A SOD1 was excluded from the nuclei of immortalized NSC34

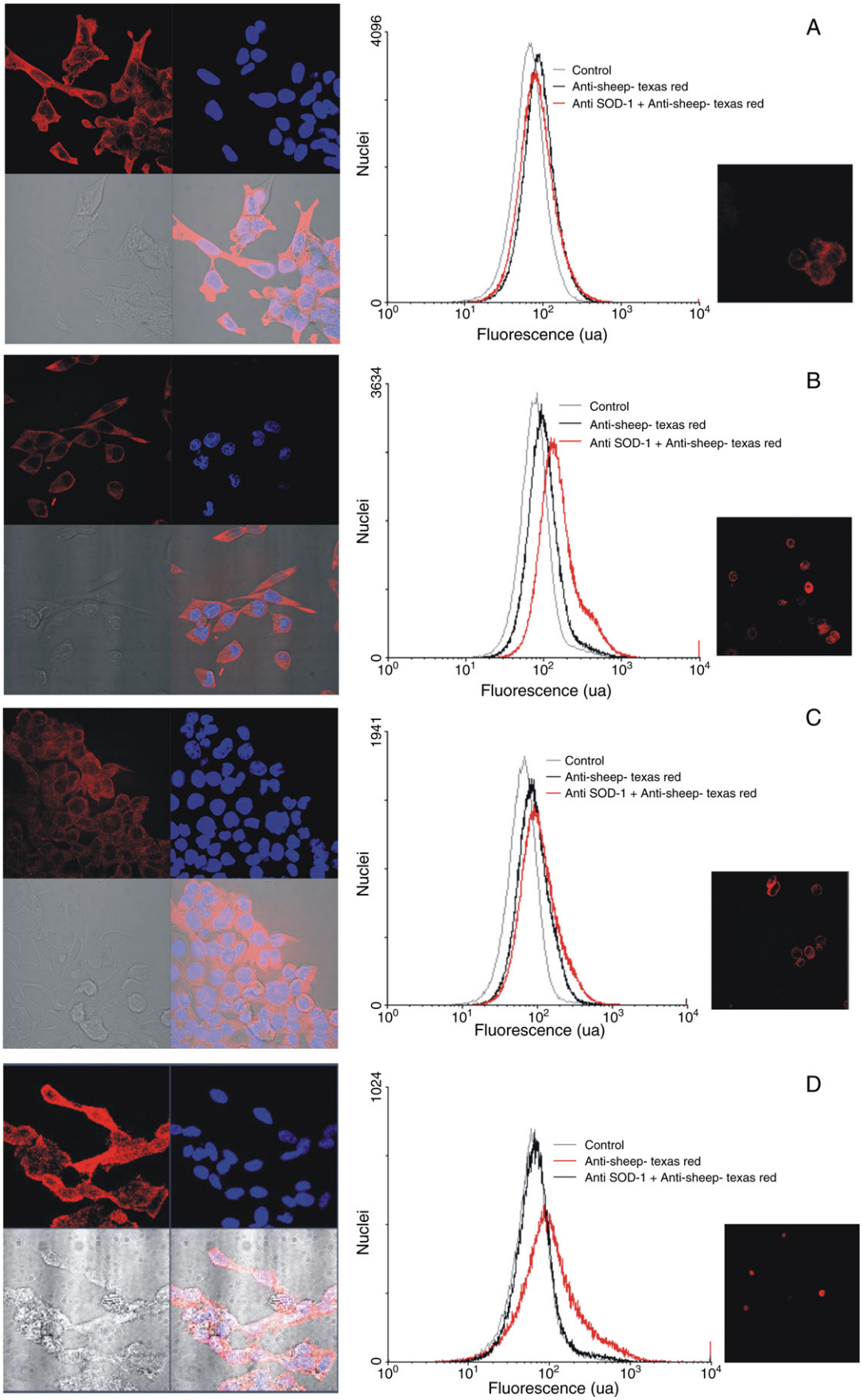

Fig. 5. Immunofluorescence and flow cytometry results of (A) SH-SY5Y; (B) WT; (C) G93A and (D) H46R. Left panel presents confocal images showing nuclei stained with DAPI (blue) and Texas Red labeled anti-SOD1 antibody (red). Right panel presents confocal images of nuclei stained with Texas Red labeled anti-SOD1 and representative FACS plots of nuclei in the absence of antibody (grey line), nuclei only with secondary antibody (black line) and nuclei with primary and secondary antibodies (red line).

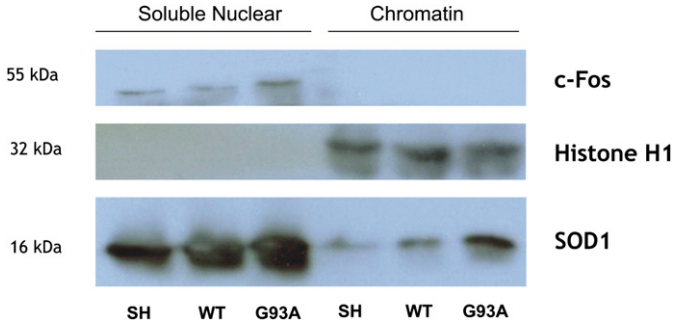

Fig. 6. Western blot analysis of soluble nuclear proteins (Soluble Nuclear) and proteins attached to the DNA (Chromatin) obtained from parental SH-SY5Y cells (SH), and from cells transfected with the wild-type SOD1 (WT) or the G93A mutant SOD1 (G93A). The c-Fos nuclear marker and the Histone H1 chromatin marker were used to assess protein loading and the purity of the fractions.

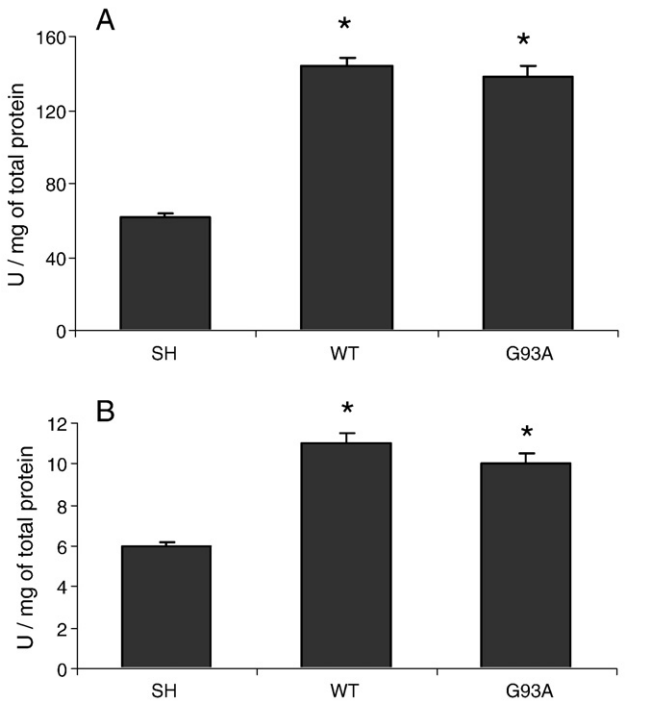

Fig. 7. Superoxide dismutase activity in cytosolic (A) and nuclear (B) extracts obtained from parental SH-SY5Y cells (SH), and from cells transfected with the wild-type SOD1 (WT) or the G93A mutant SOD1 (G93A). One SOD1 unit was defined as the amount of protein extract that promoted 50% inhibition in the rate of NBT reduction, as assessed by absorbance at 560 nm. *Significantly different from SH ($p<0.001$).

mouse motor neurons in culture. This discrepancy may be due to the high levels of human SOD1 expression in the murine cells used by these authors. The human neuroblastoma cell line (SH-SY5Y) used in the present work displayed only twice the normal SOD1 content. In SH-SY5Y cells, SOD1 could also be isolated with the chromatin proteins (Fig. 6). Contamination the chromatin protein fraction with soluble nuclear protein is very unlikely, since the protocol clearly assured sequestering of proteins tightly bound to DNA, such as histones and did not result in isolation of Fos transcription factor. Therefore, SOD1 associated with chromatin was observed for the first time, suggesting that it interacts strongly with DNA. Moreover, the level of G93A SOD1 in chromatin was greater than that of wild-type SOD1, which may indicate that the mutant SOD1 has increased affinity for DNA.

3.4. Superoxide dismutase and peroxidase activity in the nucleus

Next, we compared the enzymatic activity of SOD1 in the cytosolic and nuclear protein extracts of all three cell types (Figs. 7 and 8). Cells transfected with either wild-type (WT) or mutant SOD1 (G93A) showed increased (approximately 2-fold) superoxide dismutase activity compared to control (SH) cells in both in the cytosol and nucleus (Fig. 7A and B), in agreement with the augmented expression of SOD1 in G93A and WT cells [37]. Peroxidase activity in these neuroblastoma cells was monitored by oxidation of DHR upon addition of H_2O_2 in the presence and absence of bicarbonate (Fig. 8). The results show increased peroxidase activity in cytosolic extracts from G93A cells by 1.5 and 3-fold when compared to WT and SH cytosolic extracts, respectively (Fig. 8A). Increased peroxidase activity by 2 and 3-fold was also observed in nuclear extracts obtained from G93A cells compared to WT and SH nuclear extracts, respectively (Fig. 8B). This bicarbonate-dependent peroxidase activity is most likely due to SOD1 [43] because the participation of redox-active transition-metal was eliminated by the presence of DTPA in the assays, and because the activity of other peroxidases is not modulated by bicarbonate [44,45].

4. Discussion

Here we show accumulation of oxidative DNA damage in G93A cells as compared with SH and WT cells evaluated by 8-oxodGuo levels measured by HPLC/EC. To gain insights into the nature of oxidant species produced in cells, DNA damage was also evaluated by the Comet Assay, quantifying DNA strand breaks in the presence and absence of Fpg, a DNA glycosylase that recognizes the oxidized purine 8-oxoGua, as well as ring-opened purines or Endo III that converts oxidized pyrimidines to strand breaks [46]. The ratio of strand breaks, Fpg- and Endo III-sensitive lesions in G93A cells (1:3:3) indicates that more than one species contribute to DNA oxidation. They are likely to be the hydroxyl radical and the carbonate radical because these species present a complementary profile of DNA damage. The hydroxyl radical produces high yields of strand breaks and similar yields of oxidized purines and pyrimidines (2.5:1:1) [47,48] whereas the carbonate radical renders low yields of both strand breaks and pyrimidine oxidation [49].

The activity of DNA repair enzymes in ALS patients has been shown to be lower [50] or higher [51,52] than that of normal individuals. Although contradictory, these studies support that DNA damage may be an upstream event in motor neuron degeneration associated with ALS. Several studies have implicated apoptotic pathways in the pathogenesis of ALS, reviewed in [53,54]. The involvement of p53 protein in these pathways has also been suggested [29–31]. Ciriolo et al. previously showed that G93A cells display increased markers of apoptosis (DNA fragmentation, cytochrome *c* release, Bcl-2 immunoreactivity and caspase 3 activity), when compared to SH and WT cells [55]. Elevated levels of p53 protein have also been shown in G93A cells [55]. Here we show that accumulation of oxidative DNA damage in G93A cells activates p53 protein, thereby triggering apoptosis. These results suggest a role for the accumulation of oxidative DNA damage and p53 activation in the mechanism of motor neuron death in ALS.

The presence of SOD1 in the nucleus of mammalian cells has been previously described [39–41]. Our results confirmed this result in both G93A and H46R cells by FACS and confocal microscopy analysis. In addition, imunoblots of the chromatin fraction demonstrated for the first time that SOD1 is closely associated with DNA. These facts make it possible to correlate the mutant SOD1 with the increased levels of DNA damage observed in G93A cells. Once associated to DNA, the G93A SOD1 may directly promote DNA damage, possibly via generation of oxidants by the mutant enzyme. We showed that nuclear G93A SOD1 is active as superoxide dismutase and has increased peroxidase activity *in vivo*, when compared to wild-type SOD1. The increased levels of DNA damage observed upon H_2O_2

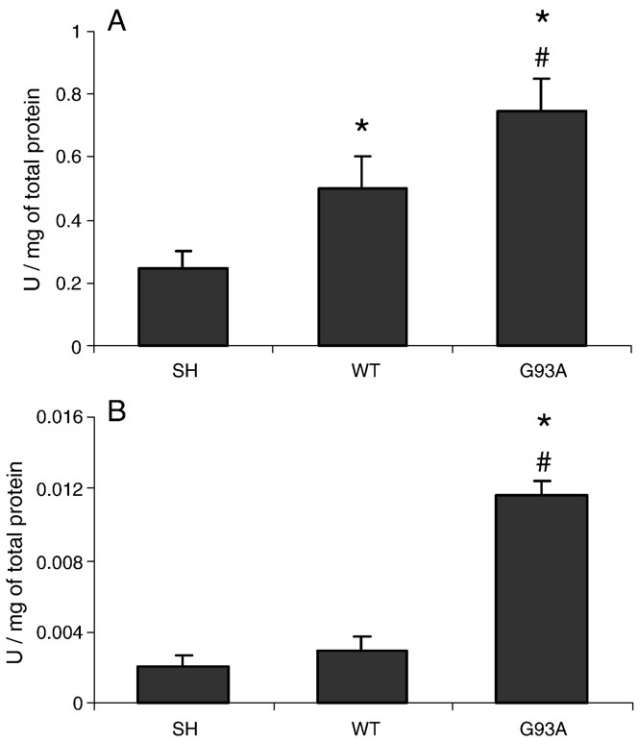

Fig. 8. Peroxidase activity in cytosolic (A) and nuclear (B) extracts obtained from parental SH-SY5Y cells (SH), and from cells transfected with the wild-type SOD1 (WT) or the G93A mutant SOD1 (G93A). One peroxidase unit was defined as the amount of protein extract that promoted rhodamine formation at a rate of 1 μM/min, as assessed by absorbance at 500 nm. To determine peroxidase activity, the rate of DHR oxidation in the absence of bicarbonate was deducted from the rate of DHR oxidation in the presence of bicarbonate. Significantly different from *SH or #WT ($p < 0.001$).

treatment were higher in G93A cells, which may also indicate augmented peroxidase activity of the mutant SOD1 present in the nucleus. Increased levels of DNA damage in ALS subjects and in animal models have been previously described [32–36]. We propose that the DNA damage observed in our cellular model could be a direct result of SOD1 peroxidase activity.

It should be noted that purified wild-type and G93A mutant SOD1 possess the same superoxide dismutase [56] and bicarbonate-dependent peroxidase activities [57]. In cellular environments and upon binding to biomolecules, however, these activities may change in an unpredictable manner. Our results show that, in a human cellular model, the FALS-mutant G93A SOD1 possesses increased peroxidase activity in both the cytosol and nucleus. G93A cells display increased (2-fold) intracellular generation of reactive oxygen species when compared to SH and WT cells, as previously suggested using DCF intracellular oxidation [55,58]. However, DCF oxidation is not specific for SOD1 peroxidase activity, while DHR oxidation in the presence of bicarbonate, shown here, is more specific. Analysis of cytosolic and nuclear extracts allowed us to gather important information about SOD1 peroxidase activity in different cellular compartments, indicative of different molecular targets for SOD1 peroxidase activity, such as DNA.

The molecular events leading to motor neuron death in ALS remains unknown, and the involvement of mutant SOD1 in these processes remains poorly understood. The toxicity of FALS-mutant SOD1 has been largely associated with its recruitment to the mitochondria [17–19] and endoplasmic reticulum (ER) [24,25]. In the present work, we propose that recruitment of FALS-mutant SOD1 to the nucleus may be as toxic as is recruitment to the mitochondria and ER since it can promote DNA damage and trigger apoptosis via p53 activation (Scheme 1). DNA damage may play an important role in the mechanism of motor neuron death observed in

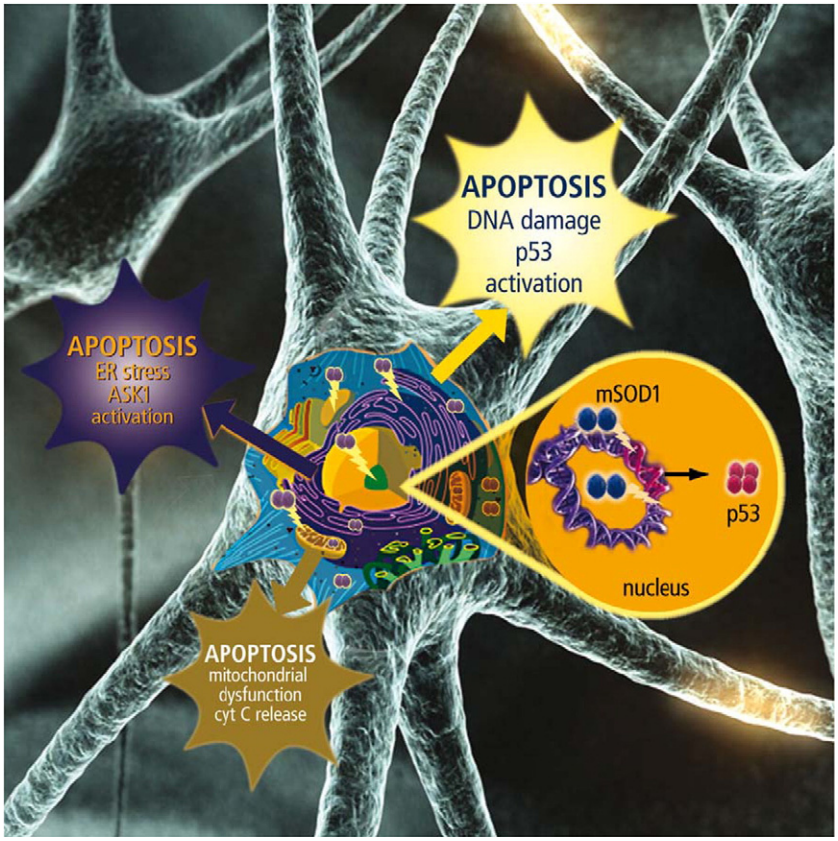

Scheme 1. Proposed mechanisms of mutant SOD1 toxicity in mitochondria [16,17], endoplasmic reticulum (ER) [23,24] and in the nucleus of a motor neuron cell.

ALS patients, and the interaction of mutant and wild-type SOD1 with DNA deserves further investigation since it could provide new insight into the complex connection between SOD1 and ALS pathogenesis.

Acknowledgements

This work was supported by the Fundação de Amparo à Pesquisa do Estado de São Paulo - FAPESP (Brazil), the Conselho Nacional para o Desenvolvimento Científico e Tecnológico – CNPq, Instituto do Milênio - Redoxoma (Brazil), Financiadora de Estudos e Projetos – FINEP (Brazil), INCT de Processos Redox em Biomedicina, Pró-Reitoria de Pesquisa da Universidade de São Paulo (Brazil), and the Italian Ministry of Health, PF 'Meccanismi molecolari e cellulari delle malattie neurodegenerative del sistema motorio' (Italy). We would like to thank Osmar Gomes and Marcos Demasi (IQ-USP, São Paulo, Brazil) for their excellent assistance. We are grateful to Dr. Luis Barbeito from Instituto Clemente Estable (Uruguay) for many helpful discussions.

References

[1] J. Charcot, A. Joffroy, Deux cas d'atrophie musculaire progressive avec lésion de la substance grise et des faisceaux antéro-latéraux de la moelle épinière, Arch. Physiol. Neurol. Path. 2 (1869) 744–754.
[2] D.W. Mulder, Clinical limits of amyotrophic lateral sclerosis, Adv. Neurol. 36 (1982) 15–22.
[3] J.F. Kurtzke, Risk factors in amyotrophic lateral sclerosis, Adv. Neurol. 56 (1991) 245–270.
[4] D.R. Rosen, T. Siddique, D. Patterson, D.A. Figlewicz, P. Sapp, A. Hentati, D. Donaldson, J. Goto, J.P. O'Regan, H.X. Deng, et al., Mutations in Cu/Zn superoxide dismutase gene are associated with familial amyotrophic lateral sclerosis, Nature 362 (1993) 59–62.
[5] P.M. Andersen, Amyotrophic lateral sclerosis associated with mutations in the CuZn superoxide dismutase gene, Curr. Neurol. Neurosci. Rep. 6 (2006) 37–46.
[6] D.R. Borchelt, M.K. Lee, H.S. Slunt, M. Guarnieri, Z.S. Xu, P.C. Wong, R.H. Brown, D.L. Price, S.S. Sisodia, D.W. Cleveland, Superoxide dismutase 1 with mutations linked to familial amyotrophic lateral sclerosis possesses significant activity, Proc. Natl. Acad. Sci. U. S. A. 91 (1994) 8292–8296.
[7] S. Rabizadeh, E.B. Gralla, D.R. Borchelt, R. Gwinn, J.S. Valentine, S. Sisodia, P. Wong, M. Lee, H. Hahn, D.E. Bredesen, Mutations associated with amyotrophic lateral sclerosis convert superoxide dismutase from an antiapoptotic gene to a proapoptotic gene: studies in yeast and neural cells, Proc. Natl. Acad. Sci. U. S. A. 92 (1995) 3024–3028.
[8] M.E. Gurney, H. Pu, A.Y. Chiu, M.C. Dal Canto, C.Y. Polchow, D.D. Alexander, J. Caliendo, A. Hentati, Y.W. Kwon, H.X. Deng, et al., Motor neuron degeneration in mice that express a human Cu,Zn superoxide dismutase mutation, Science 264 (1994) 1772–1775.
[9] C. Bendotti, M.T. Carri, Lessons from models of SOD1-linked familial ALS, Trends Mol. Med. 10 (2004) 393–400.
[10] A.G. Reaume, J.L. Elliott, E.K. Hoffman, N.W. Kowall, R.J. Ferrante, D.F. Siwek, H.M. Wilcox, D.G. Flood, M.F. Beal, R.H. Brown, R.W. Scott, W.D. Snider, Motor neurons in Cu/Zn superoxide dismutase-deficient mice develop normally but exhibit enhanced cell death after axonal injury, Nat. Genet. 13 (1996) 43–47.
[11] M. Cozzolino, A. Ferri, M.T. Carri, Amyotrophic lateral sclerosis: from current developments in the laboratory to clinical implications, Antioxid. Redox Signal. 10 (2008) 405–443.
[12] M.Y. Sherman, A.L. Goldberg, Cellular defenses against unfolded proteins: a cell biologist thinks about neurodegenerative diseases, Neuron 29 (2001) 15–32.
[13] M.D. Kirkitadze, G. Bitan, D.B. Teplow, Paradigm shifts in Alzheimer's disease and other neurodegenerative disorders: the emerging role of oligomeric assemblies, J. Neurosci. Res. 69 (2002) 567–577.
[14] H.A. Lashuel, D. Hartley, B.M. Petre, T. Walz, P.T. Lansbury, Neurodegenerative disease: amyloid pores from pathogenic mutations, Nature 418 (2002) 291.
[15] D.M. Medinas, G. Cerchiaro, D.F. Trindade, O. Augusto, The carbonate radical and related oxidants derived from bicarbonate buffer, IUBMB Life 59 (2007) 255–262.
[16] S.C. Barber, R.J. Mead, P.J. Shaw, Oxidative stress in ALS: a mechanism of neurodegeneration and a therapeutic target, Biochim. Biophys. Acta 1762 (2006) 1051–1067.
[17] A. Ferri, M. Cozzolino, C. Crosio, M. Nencini, A. Casciati, E.B. Gralla, G. Rotilio, J.S. Valentine, M.T. Carri, Familial ALS-superoxide dismutases associate with mitochondria and shift their redox potentials, Proc. Natl. Acad. Sci. U. S. A. 103 (2006) 13860–13865.
[18] J. Liu, C. Lillo, P.A. Jonsson, C. Vande Velde, C.M. Ward, T.M. Miller, J.R. Subramaniam, J.D. Rothstein, S. Marklund, P.M. Andersen, T. Brannstrom, O. Gredal, P.C. Wong, D.S. Williams, D.W. Cleveland, Toxicity of familial ALS-linked SOD1 mutants from selective recruitment to spinal mitochondria, Neuron 43 (2004) 5–17.
[19] C.M. Higgins, C. Jung, H. Ding, Z. Xu, Mutant Cu, Zn superoxide dismutase that causes motoneuron degeneration is present in mitochondria in the CNS, J. Neurosci. 22 (2002) RC215.
[20] F.R. Wiedemann, K. Winkler, A.V. Kuznetsov, C. Bartels, S. Vielhaber, H. Feistner, W.S. Kunz, Impairment of mitochondrial function in skeletal muscle of patients with amyotrophic lateral sclerosis, J. Neurol. Sci. 156 (1998) 65–72.
[21] C. Jung, C.M. Higgins, Z. Xu, Mitochondrial electron transport chain complex dysfunction in a transgenic mouse model for amyotrophic lateral sclerosis, J. Neurochem. 83 (2002) 535–545.
[22] P. Pasinelli, M.E. Belford, N. Lennon, B.J. Bacskai, B.T. Hyman, D. Trotti, R.H. Brown, Amyotrophic lateral sclerosis-associated SOD1 mutant proteins bind and aggregate with Bcl-2 in spinal cord mitochondria, Neuron 43 (2004) 19–30.
[23] H. Takeuchi, Y. Kobayashi, S. Ishigaki, M. Doyu, G. Sobue, Mitochondrial localization of mutant superoxide dismutase 1 triggers caspase-dependent cell death in a cellular model of familial amyotrophic lateral sclerosis, J. Biol. Chem. 277 (2002) 50966–50972.
[24] D. Kieran, I. Woods, A. Villunger, A. Strasser, J.H. Prehn, Deletion of the BH3-only protein puma protects motoneurons from ER stress-induced apoptosis and delays motoneuron loss in ALS mice, Proc. Natl. Acad. Sci. U. S. A. 104 (2007) 20606–20611.
[25] H. Nishitoh, H. Kadowaki, A. Nagai, T. Maruyama, T. Yokota, H. Fukutomi, T. Noguchi, A. Matsuzawa, K. Takeda, H. Ichijo, ALS-linked mutant SOD1 induces ER stress- and ASK1-dependent motor neuron death by targeting Derlin-1, Genes Dev. 22 (2008) 1451–1464.
[26] A.J. Levine, p53, the cellular gatekeeper for growth and division, Cell 88 (1997) 323–331.
[27] T. Rich, R.L. Allen, A.H. Wyllie, Defying death after DNA damage, Nature 407 (2000) 777–783.
[28] D.W. Meek, Tumor suppression by p53: a role for the DNA damage response? Nat. Rev., Cancer 9 (2009) 714–723.
[29] S.M. de la Monte, Y.K. Sohn, N. Ganju, J.R. Wands, P53- and CD95-associated apoptosis in neurodegenerative diseases, Lab. Invest. 78 (1998) 401–411.
[30] J.L. Gonzalez de Aguilar, J.W. Gordon, F. Rene, M. de Tapia, B. Lutz-Bucher, C. Gaiddon, J.P. Loeffler, Alteration of the Bcl-x/Bax ratio in a transgenic mouse model of amyotrophic lateral sclerosis: evidence for the implication of the p53 signaling pathway, Neurobiol. Dis. 7 (2000) 406–415.
[31] L.J. Martin, p53 is abnormally elevated and active in the CNS of patients with amyotrophic lateral sclerosis, Neurobiol. Dis. 7 (2000) 613–622.
[32] N. Aguirre, M.F. Beal, W.R. Matson, M.B. Bogdanov, Increased oxidative damage to DNA in an animal model of amyotrophic lateral sclerosis, Free Radic. Res. 39 (2005) 383–388.
[33] R.J. Ferrante, S.E. Browne, L.A. Shinobu, A.C. Bowling, M.J. Baik, U. MacGarvey, N.W. Kowall, R.H. Brown, M.F. Beal, Evidence of increased oxidative damage in both sporadic and familial amyotrophic lateral sclerosis, J. Neurochem. 69 (1997) 2064–2074.
[34] P.S. Fitzmaurice, I.C. Shaw, H.E. Kleiner, R.T. Miller, T.J. Monks, S.S. Lau, J.D. Mitchell, P.G. Lynch, Evidence for DNA damage in amyotrophic lateral sclerosis, Muscle Nerve 19 (1996) 797–798.
[35] Y. Ihara, K. Nobukuni, H. Takata, T. Hayabara, Oxidative stress and metal content in blood and cerebrospinal fluid of amyotrophic lateral sclerosis patients with and without a Cu, Zn-superoxide dismutase mutation, Neurol. Res. 27 (2005) 105–108.
[36] M. Bogdanov, R.H. Brown, W. Matson, R. Smart, D. Hayden, H. O'Donnell, M.F. Beal, M. Cudkowicz, Increased oxidative damage to DNA in ALS patients, Free Radic. Biol. Med. 29 (2000) 652–658.
[37] M.T. Carri, A. Ferri, A. Battistoni, L. Famhy, R. Gabbianelli, F. Poccia, G. Rotilio, Expression of a Cu, Zn superoxide dismutase typical of familial amyotrophic lateral sclerosis induces mitochondrial alteration and increase of cytosolic Ca^{2+} concentration in transfected neuroblastoma SH-SY5Y cells, FEBS Lett. 414 (1997) 365–368.
[38] I. Nicoletti, G. Migliorati, M.C. Pagliacci, F. Grignani, C. Riccardi, A rapid and simple method for measuring thymocyte apoptosis by propidium iodide staining and flow cytometry, J. Immunol. Methods 139 (1991) 271–279.
[39] L.Y. Chang, J.W. Slot, H.J. Geuze, J.D. Crapo, Molecular immunocytochemistry of the CuZn superoxide dismutase in rat hepatocytes, J. Cell Biol. 107 (1988) 2169–2179.
[40] R. Del Maestro, W. McDonald, Subcellular localization of superoxide dismutases, glutathione peroxidase and catalase in developing rat cerebral cortex, Mech. Ageing Dev. 48 (1989) 15–31.
[41] J.W. Slot, H.J. Geuze, B.A. Freeman, J.D. Crapo, Intracellular localization of the copper–zinc and manganese superoxide dismutases in rat liver parenchymal cells, Lab. Invest. 55 (1986) 363–371.
[42] D. Sau, S. De Biasi, L. Vitellaro-Zuccarello, P. Riso, S. Guarnieri, M. Porrini, S. Simeoni, V. Crippa, E. Onesto, I. Palazzolo, P. Rusmini, E. Bolzoni, C. Bendotti, A. Poletti, Mutation of SOD1 in ALS: a gain of a loss of function, Hum. Mol. Genet. 16 (2007) 1604–1618.
[43] H. Zhang, C. Andrekopoulos, J. Joseph, K. Chandran, H. Karoui, J.P. Crow, B. Kalyanaraman, Bicarbonate-dependent peroxidase activity of human Cu, Zn-superoxide dismutase induces covalent aggregation of protein: intermediacy of tryptophan-derived oxidation products, J. Biol. Chem. 278 (2003) 24078–24089.
[44] Y.M. Kim, J.M. Lim, B.C. Kim, S. Han, Cu, Zn-superoxide dismutase is an intracellular catalyst for the H_2O_2-dependent oxidation of dichlorodihydrofluorescein, Mol. Cells 21 (2006) 161–165.
[45] H. Zhang, J. Joseph, M. Gurney, D. Becker, B. Kalyanaraman, Bicarbonate enhances peroxidase activity of Cu, Zn-superoxide dismutase. Role of carbonate anion radical and scavenging of carbonate anion radical by metalloporphyrin antioxidant enzyme mimetics, J. Biol. Chem. 277 (2002) 1013–1020.
[46] A.R. Collins, A.A. Oscoz, G. Brunborg, I. Gaivao, L. Giovannelli, M. Kruszewski, C.C. Smith, R. Stetina, The comet assay: topical issues, Mutagenesis 23 (2008) 143–151.

[47] J. Cadet, T. Douki, J.L. Ravanat, Oxidatively generated damage to the guanine moiety of DNA: mechanistic aspects and formation in cells, Acc. Chem. Res. 41 (2008) 1075–1083.
[48] J.P. Pouget, T. Douki, M.J. Richard, J. Cadet, DNA damage induced in cells by gamma and UVA radiation as measured by HPLC/GC-MS and HPLC-EC and Comet assay, Chem. Res. Toxicol. 13 (2000) 541–549.
[49] Y.A. Lee, B.H. Yun, S.K. Kim, Y. Margolin, P.C. Dedon, N.E. Geacintov, V. Shafirovich, Mechanisms of oxidation of guanine in DNA by carbonate radical anion, a decomposition product of nitrosoperoxycarbonate, Chem.- Eur. J. 13 (2007) 4571–4581.
[50] G.E. Kisby, J. Milne, C. Sweatt, Evidence of reduced DNA repair in amyotrophic lateral sclerosis brain tissue, Neuroreport 8 (1997) 1337–1340.
[51] S.H. Kim, J.I. Engelhardt, J.S. Henkel, L. Siklos, J. Soos, C. Goodman, S.H. Appel, Widespread increased expression of the DNA repair enzyme PARP in brain in ALS, Neurology 62 (2004) 319–322.
[52] A.Y. Shaikh, L.J. Martin, DNA base-excision repair enzyme apurinic/apyrimidinic endonuclease/redox factor-1 is increased and competent in the brain and spinal cord of individuals with amyotrophic lateral sclerosis, Neuromol. Med. 2 (2002) 47–60.
[53] S. Sathasivam, P.J. Shaw, Apoptosis in amyotrophic lateral sclerosis—what is the evidence? Lancet Neurol. 4 (2005) 500–509.
[54] S.R. Bacman, W.G. Bradley, C.T. Moraes, Mitochondrial involvement in amyotrophic lateral sclerosis: trigger or target? Mol. Neurobiol. 33 (2006) 113–131.
[55] M.R. Ciriolo, A. De Martino, E. Lafavia, L. Rossi, M.T. Carri, M.T.G. Rotilio, Cu, Zn-superoxide dismutase-dependent apoptosis induced by nitric oxide in neuronal cells, J. Biol. Chem. 275 (2000) 5065–5072.
[56] M.B. Yim, J.H. Kang, H.S. Yim, H.S. Kwak, P.B. Chock, E.R. Stadtman, A gain-of-function of an amyotrophic lateral sclerosis-associated Cu, Zn-superoxide dismutase mutant: an enhancement of free radical formation due to a decrease in Km for hydrogen peroxide, Proc. Natl. Acad. Sci. U. S. A. 93 (1996) 5709–5714.
[57] R.J. Singh, H. Karoui, M.R. Gunther, J.S. Beckman, R.P. Mason, B. Kalyanaraman, Reexamination of the mechanism of hydroxyl radical adducts formed from the creaction between familial amyotrophic lateral sclerosis-associated Cu, Zn superoxide dismutase mutants and H2O2, Proc. Natl. Acad. Sci. U. S. A. 95 (1998) 6675–6680.
[58] S. Beretta, G. Sala, L. Mattavelli, C. Ceresa, A. Casciati, A. Ferri, M.T. Carri, C. Ferrarese, Mitochondrial dysfunction due to mutant copper/zinc superoxide dismutase associated with amyotrophic lateral sclerosis is reversed by N-acetylcysteine, Neurobiol. Dis. 13 (2003) 213–221.